EFFECTS OF ENERGY WINDOW WIDTH ON PLANAR IMAGE QUALITY OF THYROID IMAGING USING SINGLE-HEADED GAMMA CAMERA

NUR LIYANA BINTI JAMSARI

DEGREE IN BACHELOR OF HEALTH SCIENCES

(MEDICAL RADIATION)

UNIVERSITI SAINS MALAYSIA

2015

CERTIFICATE

This is to certify that the dissertation entitled

"Effects of Energy Window Width on Planar Image Quality of Thyroid Imaging using Single-Headed Gamma Camera"

Is the bona fide record of research work done by

NUR LIYANA BINTI JAMSARI (112331)

During the period September 2014 to June 2015

Under our supervision

Supervisor,

..... .

Madam Chen Suk Chiang
Lecturer of Medical Radiation
School of Health Sciences,
Universiti Sains Malaysia,
16150 KubangKerian,
Kelantan, Malaysia.
Date: .....

Co-Supervisor,

.....

Mr Abdullah Waidi Bin Haji Idris
Supervisor of Medical Radiation,
School of Health Sciences,
Universiti Sains Malaysia,
16150 KubangKerian,
Kelantan, Malaysia.
Date: .....

Effects of Energy Window Width on Planar Image Quality of Thyroid Imaging using Single-Headed Gamma Camera

by

NUR LIYANA BINTI JAMSARI

Dissertation submitted in partial fulfillment

of the requirement for the degree

of Bachelor of Health Sciences (Medical Radiation)

June 2015

ACKNOWLEDGEMENT

My gratitude to the almighty Allah for His blessing and giving me strength and patience to complete my undergraduate research project. I would like to express the deepest appreciation to my beloved supervisor, Madam Chen Suk Chiang, who had continually and convincingly conveyed spirit of adventure and excitement in regard to research. She showed me different ways to approach a research problem and the important to be persistent to accomplish my goal. Without her guidance and patience in helping me, this dissertation would not have been possible to complete.

To my co-supervisor, Mr Abdullah Waidi, thank you very much for your guidance and patience especially during my data collection and analyze data in Nuclear Medicine Department of Hospital Universiti Sains Malaysia. I also would like to thank Head Department of Nuclear Medicine, Oncology and Radiotherapy, Dr Lutfi, for letting me to use various equipments in that department and also gave permission for me to complete my research.

Special thanks go to my dearest friends, Murshidah Binti Mat Hazir, Nur Amalena Husna Binti Zulkepli, Nor Fadhilah Binti Ahamad and Siti Nur Amalina Binti Mustapha for your help during my research and writing. Not forgotten to my lecturers and friends in Medical Radiation program for their guide, help and support.

Last but not least, I would like to express my indebtness to my beloved parents, Mr Jamsari Bin Awang and Mrs. Anisah Binti Abdullah and to my brothers and sisters for their encouragement and support.

TABLE OF CONTENTS

LIST OF TABLES

LIST OF FIGURES

LIST OF PLATES

LIST OF SYMBOLS AND ABBREVIATIONS

SNR	Signal to noise ratio
PHA	Pulse height analyzer
LEHR	Low energy high resolution collimator
Tc-99m	Technetium-99m
mCi	miliCurie
SPECT	Single photon emission tomography
keV	kiloelectron voltage
C-D	Contrast-Detail
T_3	Tri-iodothyronine
T_4	Tetra-iodothyronine
I-131	Iodine-131
I-123	Iodine-123
A	Activity
A_0	Initial activity
Λ	Decay constant
t	Time
HC	Hot contrast
CC	Cold contrast

N_N	Mean number of counts per pixel in nodule
N_B	Mean number of counts per pixel in background
μ	Mean counts
σ	Standard deviation
H1	Hot nodule 1
H2	Hot nodule 2
C1	Cold nodule 1
C2	Cold nodule 2
ROI	Region of interest

ABSTRACT

The aim of this study is to evaluate the effects of energy window width on the planar image quality of thyroid phantom. The values of contrast and signal to noise ratio (SNR) were evaluated in this study. It was carried out by using a thyroid phantom that had been filled with 5.566 mCi Tc-99m radioactive sources. A static image of the thyroid phantom was captured using the single-headed gamma camera (Symbia-E) at five different energy window widths of 10%, 15%, 20%, 30% and 40% which was equipped with LEHR collimator, stopping condition 300 kilocounts and matrix size of 128 × 128. The average counts obtained were recorded in a table and the contrast and SNR for hot and cold nodules were calculated using the given equation. For contrast, 15% energy window width gave the highest values for the hot nodules but for the cold nodules, it gave lower contrast values compared to 40%. However, the cold nodule at 15% energy window width gave the higher contrast values than 10%, 20% and 30% energy window widths. For SNR, the energy window width of 15% gave the highest values at all four nodules (two hot nodules and two cold nodules). Therefore, the optimum energy window width was the 15% for Tc-99m radioactive and planar imaging for thyroid.

ABSTRAK

Tujuan kajian ini adalah untuk menilai kesan *energy window width* kepada kualiti imej satah fantom tiroid. Nilai-nilai kontras dan nisbah isyarat kepada bunyi (SNR) telah dinilai dalam kajian ini. Ia dilakukan dengan menggunakan fantom tiroid yang telah dipenuhi dengan sumber radioaktif sebanyak 5.566 mCi Tc-99m. Satu imej statik fantom tiroid ditangkap menggunakan kamera gamma berkepala tunggal (Symbia-E) pada lima *energy window widths* yang berbeza, iaitu 10%, 15%, 20%, 30% dan 40% yang dilengkapi dengan pelapis LEHR, berhenti keadaan 300 kilocounts dan saiz matriks 128 × 128. Kontras dan SNR untuk nodul panas dan sejuk telah dikira dengan menggunakan persamaan yang diberikan dan kiraan purata yang diperolehi telah direkodkan dalam jadual. Untuk kontras, 15% *energy window width* memberikan nilai tertinggi bagi nodul panas tetapi untuk nodul sejuk, ia memberikan nilai kontras yang lebih rendah berbanding dengan 40%. Walau bagaimanapun, nodul sejuk pada 15% *energy window width* memberikan nilai kontras yang lebih tinggi daripada 10%, 20% dan 30% *energy window widths*. Untuk SNR, *energy window width* 15% memberi nilai tertinggi di keempat-empat nodul (dua nodul panas dan dua nodul sejuk). Oleh itu, *energy window width* yang optimum adalah 15% untuk Tc-99m radioaktif dan satah pengimejan untuk tiroid.

CHAPTER 1

INTRODUCTION

1.1 BACKGROUND OF STUDY

1.1.1 Thyroid gland

Thyroid gland is one of endocrine glands which in butterfly-shaped. It is lying in the neck which is at the front of the upper part of the trachea and between the thyroid cartilage and sterna notch. This gland is relatively small which has two lobes that are connected in the middle by the isthmus.

The main function of thyroid gland is to synthesize, store and secrete hormones (Crawford *et al.*, 2009). There are two types of hormones that produced by thyroid gland which are iodine-containing hormones (tri-iodothyronine, T_3 and tetra-iodothyronine, T_4) and polypeptide hormone (calcitonin). The thyroid gland is unique gland because it stores a large amount of hormones in an inactive form.

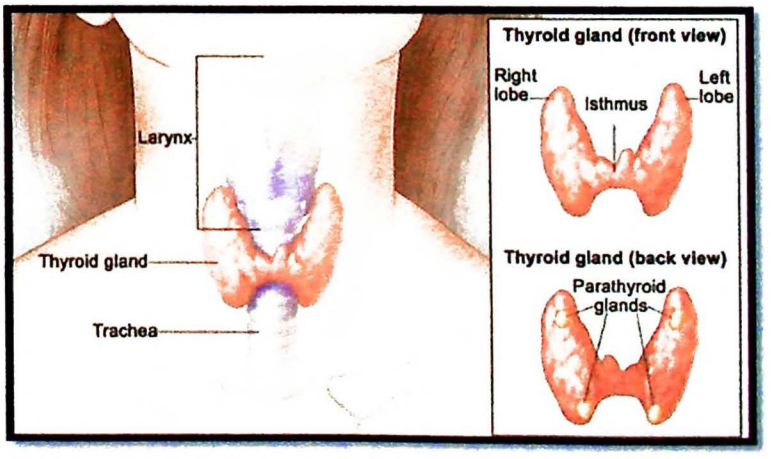

Figure 1.1 The anatomical structure of thyroid gland

1.1.2 Thyroid scintigraphy

Thyroid scintigraphy is one of imaging procedure in nuclear medicine. The procedure is done to evaluate the functions of thyroid. There are three different methods to evaluate thyroid function and structure. The methods are a thyroid scan produces an image of the thyroid gland, a radioactive iodine uptake test that measures function of thyroid without imaging and a whole-body thyroid scan (Giorgi, 2012).

Thyroid scan is done for many reasons such as to check if the gland functioning properly, to help diagnose problems that related to thyroid such as hyperthyroidism, to assess the nature of a nodule and to detect any abnormalities in thyroid or around it (Hoad-Robson & Tidy, 2012).

1.1.3 Energy window width

Window width of energy is considered as one of the most important physical parameters for enhancement of image quality and scatter events suppression in SPECT images (Alireza & Payvand, 2012). Window width of energy is considered as one of the most important physical parameters affecting the quality of planer and SPECT images (Abdelhalim *et al.*, 2009).

The energy window width is used to exclude scattered events by using pulse height analyzer (PHA) (Prekeges, 2013). The energy window width will rejects more scatter photons and decreases the counts rate. The narrow the window, the more scatter photon will reduce. This will lead to more primary photons collected and the quality of image will be increases (Alireza & Payvand, 2012).

The selection of energy is important for imaging because it gives a mean to discriminate against gamma rays that have been scattered in the body and lost their positional information. There are two different ways that can be used to select a photopeak event. Firstly is the simple energy discrimination on the Z-signal. The second method is the photopeak positions and appropriate discriminator level settings. It is computed and stored for many different locations across the detector face. But it is only suitable for digital cameras (Cherry *et al.*, 2012).

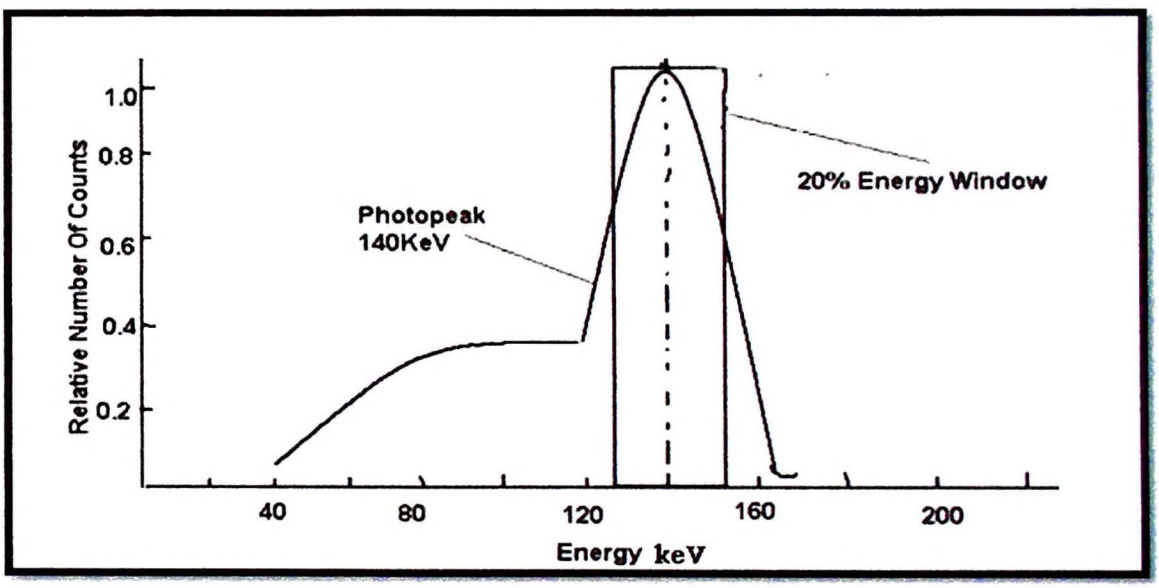

Figure 1.2 Relationship between energy of Tc-99m (keV) versus the relative number of counts

1.1.4 Planar image quality

Image quality refers to the faithfulness with which an image represents the imaged object and the quality of nuclear medicine images is limited by several factors. There are two basic methods for evaluating image quality which are physical characteristics (spatial resolution, contrast and noise) and by means of observer performance studies using images obtained with different imaging

systems (Contrast-Detail (C-D) studies, Receiver Operating Characteristics (ROC) studies) (Cherry *et al.*, 2012).

In planar image quality, the physical parameters that can be considered are resolution, noise and signal-noise ratio (Wang, 2014). The imaging procedure in nuclear medicine is the combination of selection of radiopharmaceutical, amount of injected radioactivity, collimator selection and time of imaging.

In order to get an optimum image quality, there are some parameters that should be considered. But, there are some difficulties because once we change one parameter; there other parameter will affect too. This is because these parameters were not independent (Harkness, 2012).

1.2 PROBLEM STATEMENT AND SIGNIFICANCE OF STUDY

The manufacturer of the Siemens Symbia-E gamma camera had suggested that 15% of energy window width will give the optimum image quality. But, in Department of Nuclear Medicine, Oncology and Radiotherapy, Hospital Universiti Sains Malaysia, they used 20% energy window width during the imaging procedures.

The significance of the study is to figure out the optimum energy window width that gives the best image quality. This also will help the medical practitioner in Hospital Universiti Sains Malaysia to get the best image quality in order to diagnose a patient with a clearer visual.

1.3 AIM AND OBJECTIVES

1.3.1 Aim of study

To evaluate the effect of energy window widths on the planar image quality of thyroid phantom.

1.3.2 Objectives of study

a) To determine the effects of different energy window widths (10%, 15%, 20%, 30% and 40%) on contrast of planar images

b) To determine the effect of different energy window widths (10%, 15%, 20%, 30% and 40%) on signal to noise ratio (SNR) of the planar images produced

c) To compare the contrast and signal to noise ratio (SNR) of different energy window widths (10%, 15%, 20%, 30% and 40%)

CHAPTER 2

LITERATURE REVIEW

Based on Abdelhalim *et al.*, (2012), the energy window width is considered as one of the most crucial physical factors which affect the image quality for planar and SPECT imaging. In their study, the best energy window width was in the range from 15% to 20%.

One of the most prominent physical parameters that affect the quality of image in SPECT and planar is window width of energy. The narrower window width rejects scatter radiations and decreases the count rate (Alireza & Payvand, 2012). In the present research, it was evident that window width of energy played a major effect on quality of image using the Tc-99m source. Several factors cause poor spatial resolution and image quality in the reconstructed nuclear medicine images such as scatter events in the patient body, collimators or scintillation crystals.

The one of main factors of error in nuclear medicine data processing was scattered photon. A lot of techniques had been introduced to increase image quality and one of it was using pulse height analyzer. This pulse height analyzer is the only way that available to discriminate primary radiations from the scattered ones. In the research, the optimum energy window width obtained was the 15% (Jabbari *et al.*, 2004).

In nuclear medicine, the appropriate choice of energy window width and the radionuclide were the key in order to get a good image quality (A *et* al., 2015). Based on Kalantari *et al.,* (2008), a low signal to noise ratio distributed to a low dose of radionuclide and the presence of scattered radiations are the main barriers.

Based on Koral *et al.*, (1986), the acceptance window had been set historically in nuclear medicine in order to maximize contrast and resolution in the image produced. For a source in air, the 20% window had been set so that the count rate will be reduced.

CHAPTER 3

MATERIALS AND METHODS

3.1 MATERIALS

3.1.1 Thyroid phantom

A thyroid phantom (model of Victoreen) with serial number of S/N 45657-020 was used in this research in order to contribute a human thyroid. This thyroid phantom permits the precise duplication of clinical conditions and it is made up of lucite. (Willoughby, 2014). It consists of four nodules which are two hot spots (6 mm and 12 mm) and two cold spots (9 mm and 13 mm). The 12 mm and 13 mm spots are located at the lower part of the phantom while the 6 mm and 9 mm spots are situated at the upper part.

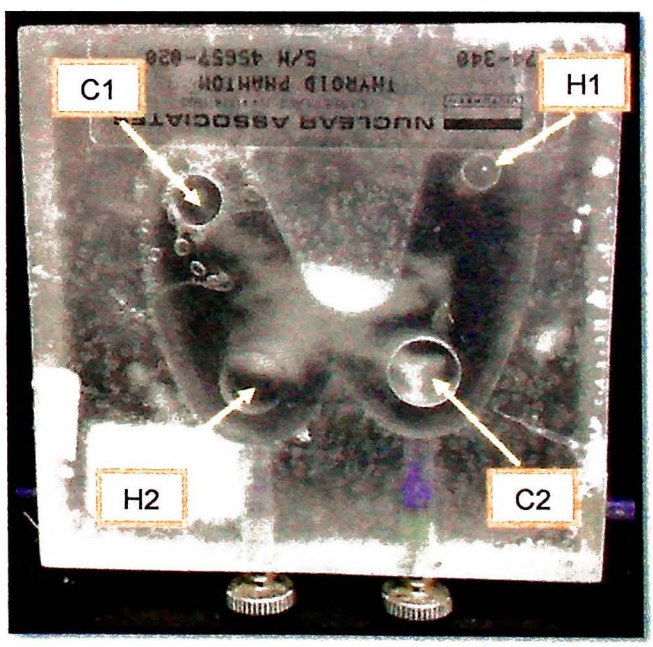

Plate 3.1 Thyroid phantom with Tc-99m

H1 = hot nodule (6 mm)

H2 = hot nodule (12 mm)

C1 = cold nodule (9 mm)

C2 = cold nodule (13 mm)

3.1.2 Radioactive source

For thyroid scintigraphy, there are three types of radioactive used which are iodine-131 (I-131), iodine-123 (I-123) and technetium-99m (Tc-99m). But the most commonly used is I-131 and Tc-99m. This is because I-123 is expensive and the production of this radioactive is also complex even though it is a good substitute for I-131 because it has a shorter half-life (13 hours). I-131 is commonly used for hyperthyroidism. But it has a disadvantage of high radiation doses to the thyroid due to the long half-life (8 days) and β^- particle emission.

In this study, the technetium-99m (Tc-99m) was used. It is commonly used in thyroid imaging such as to study the thyroid function. Other than that, Tc-99m gives a lower radiation dose because its half-life is only 6 hours and the cost is inexpensive and it is available easily. Thyroid scintigraphy using tc-99m had been proven to be more benefits compared to I-131. Using this radioactive, the image quality is better and the procedure is faster (Ramos *et al.*, 2002).

3.1.3 Gamma camera

Gamma camera is an imaging technique used to carry out functional scans such as brain, thyroid, lung, kidneys and so on. There are three terms that described primary operational characteristics of the gamma camera which are uniformity, resolution and sensitivity (Prekeges, 2013). In this study, the gamma camera used was a single-headed gamma camera (Symbia-E). It consists of a

gamma camera detector that mounted on a gantry. It allows the camera to be positioned in a flexible way.

Plate 3.2 Symbia-E single-headed gamma camera

3.1.4 Collimator

In this study, the collimator used was a low energy high resolution (LEHR). It has more holes that are smaller and deeper.

3.1.5 Syngo-Mi Workplace

The data was processed by the Syngo-Mi Workplace and it supports the entire clinical workflow by allowing the technologist to process and display the images at one workstation. As optimized image quality is obtained by applying the advanced reconstruction method, it will improve the productivity.

3.2 METHODS

3.2.1 Preparation of Tc-99m

Technetium-99m (Tc-99m) was extracted into a vial from the Molybdenum generator in sufficient volume only. This process is called elution process. The vial was put into the dose calibrator to measure the amount of activity. For this study, the activity used was 5.566 mCi.

After that, the Tc-99m was put into the thyroid phantom and water is added to fulfil the phantom. Make sure there is no bubble inside the phantom. Lastly, the phantom was left for 5 minutes to allow a uniform distribution of source within it.

The activity of radioactive was calculated by using decay factor as shown below;

$$A = A_0 e^{-\lambda t} \quad \text{——————————} \quad (1)$$

(Prekeges, 2013)

where,

A : activity

A_0 : initial activity

λ : decay constant

t : time

3.2.2 Phantom positioning

After 5 minutes, the thyroid phantom is placed under the gamma camera. The thyroid phantom is positioned as clinical condition for planar imaging and was

centered so that the phantom was in the middle of focal plane of the collimator. The angle of gamma camera is 0°.

3.2.3 Data acquisition

In this research, a Siemens Symbia E Single-headed Gamma Camera was used. This gamma camera was equipped with low-energy high resolution (LEHR) collimator. The distance of phantom to collimator was adjusted to closer as possible.

The energy window of Tc-99m was centered at 140 keV. The window width used was 15% and the peaking was performed. The view used for this procedure was anterior. A static image was acquired using a thyroid uptake acquisition mode with matrix size 128×128 with a hardware zoom of 3.2 and a stop condition of 300 kilocounts. The scanning will be done after that. The procedure is repeated by changing the window width to 20%, 30% and 40% respectively.

Table 3.1 Parameters used in the research

Parameter	Name/Value
Activity used	5.566 mCi
View of Detector	Anterior
Collimator used	LEHR
Counts	300 kilocounts
Matrix size	128×128
Zoom	3.2
Energy window width	10%, 15%, 20%, 30%, and 40%

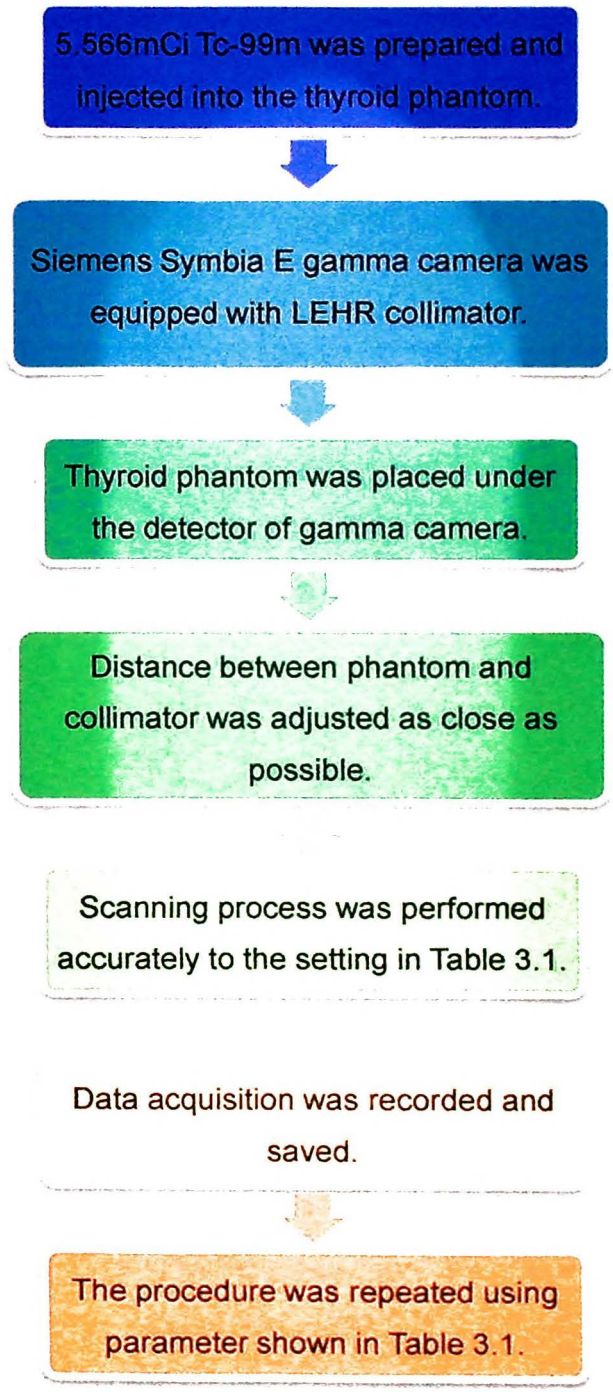

Figure 3.1 Flow chart of the full procedure in this research

3.2.4 Contrast measurement

Contrast is the charge in image intensity per incremental change in counts per pixel. It can be determined mathematically (Prekeges, 2013). The contrast of each point for each energy window width was calculated by using the below equation (Seret, 2009);

$$HC = \left(\frac{N_N}{N_B}\right) - 1 \quad \text{(2)}$$

$$CC = 1 - \left(\frac{N_N}{N_B}\right) \quad \text{(3)}$$

(Seret, 2009)

where,

CC: cold nodule/ROI (C1 and C2)

HC: hot nodule/ROI (H1 and H2)

N_N: Mean no. of counts per pixel in nodule ROI

N_B: Mean no. of counts per pixel in background ROI

3.2.5 SNR measurement

Noise is an unwanted variation in a wanted signal but most of scientists used the concept of SNR in a lot of situation. This is because we cannot detect the signal. The SNR of each point for every energy window widths were calculated using the basic formula to get SNR is shown as below (Bushberg *et al.*, 2002);

$$SNR = \frac{\mu}{\sigma} \quad \text{(4)}$$

(Bushberg *et al.*, 2002)

where,

SNR : signal-noise ratio

μ : mean counts

σ : standard deviation

3.2.6 Data collection

Number of pixels obtained at all five energy window widths (10%, 15%, 20%, 30% and 40%) was same which were16384.

Table 3.2 Average counts and standard deviation (SD) at 10% energy window width

Point	Background	Hot nodule, H1	Hot nodule, H2	Cold nodule, C1	Cold nodule, C2
Average count	180.50	55.84	92.54	204.05	261.10
Standard deviation (SD)	74.15	13.07	31.32	27.90	25.39

Table 3.3 Average counts and standard deviation (SD) at 15% energy window width

Point	Background	Hot nodule, H1	Hot nodule, H2	Cold nodule, C1	Cold nodule, C2
Average count	186.98	59.67	99.24	192.53	266.90
Standard deviation (SD)	69.42	9.63	19.79	19.72	22.84

Table 3.4 Average counts and standard deviation (SD) at 20% energy window width

Point	Background	Hot nodule, H1	Hot nodule, H2	Cold nodule, C1	Cold nodule, C2
Average count	177.07	54.93	76.84	210.00	272.42
Standard deviation (SD)	74.50	15.95	28.44	32.70	23.71

Table 3.5 Average counts and standard deviation (SD) at 30% energy window width

Point	Background	Hot nodule, H1	Hot nodule, H2	Cold nodule, C1	Cold nodule, C2
Average count	178.52	55.67	79.79	190.87	261.03
Standard deviation (SD)	70.32	13.53	20.09	19.58	22.71

Table 3.6 Average counts and standard deviation (SD) at 40% energy window width

Point	Background	Hot nodule, H1	Hot nodule, H2	Cold nodule, C1	Cold nodule, C2
Average count	238.21	72.21	85.62	199.59	249.27
Standard deviation (SD)	43.34	19.07	24.22	35.40	22.36

3.2.7 Data analysis

The images were constructed using the Syngo-Mi Workplace Software. In order to determine the optimum energy window width for thyroid planar imaging, the ability of each window width to produce a high contrast and SNR were considered as the main factors. The best energy window width would be chosen among the highest contrast and SNR for all four points.

CHAPTER 4

RESULTS

Table 4.1 showed the contrast for each nodule for every energy window widths that had been calculated (can be referred at the Appendix C). **Figure 4.1**, **Figure 4.2**, **Figure 4.3**, **Figure 4.4** and **Figure 4.5** were the graph of contrast for each energy window width respectively. The comparisons of contrast for all five energy window widths were shown in the **Figure 4.11.**

Table 4.1 Contrast values of each point for each energy window width

Energy window width (%)	Contrast			
	H1	H2	C1	C2
10	-0.691	-0.487	-0.130	-0.447
15	-0.681	-0.469	-0.030	-0.427
20	-0.690	-0.566	-0.186	-0.538
30	-0.688	-0.553	-0.069	-0.462
40	-0.697	-0.641	0.162	-0.046

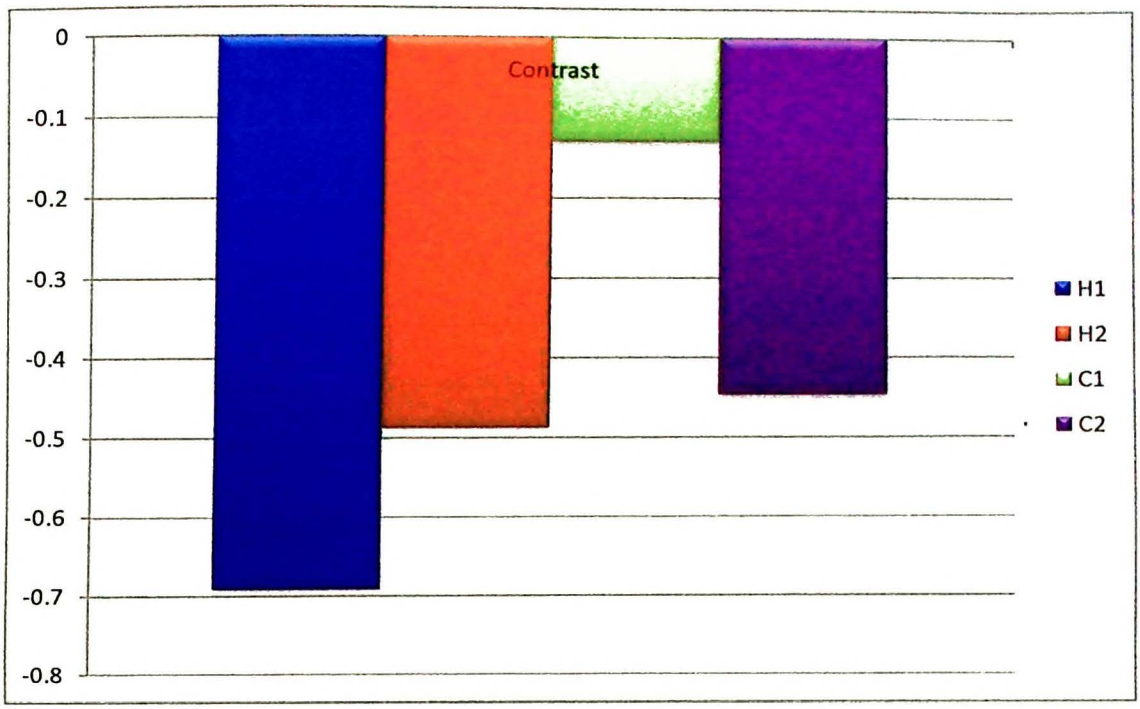

Figure 4.1 Contrast values for 10% energy window width

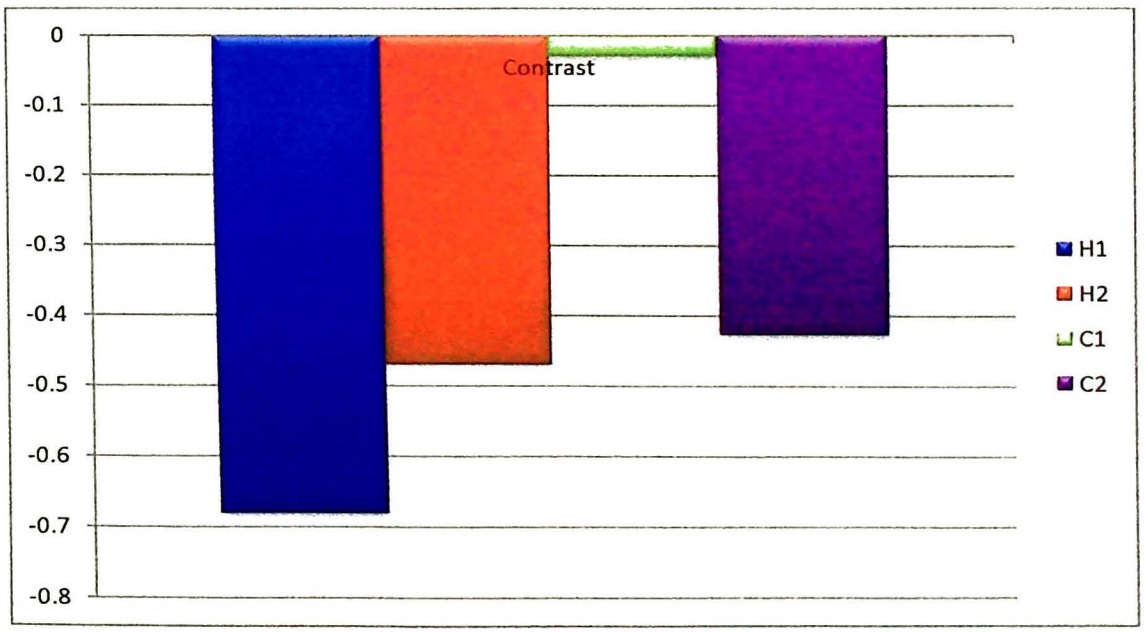

Figure 4.2 Contrast values for 15% energy window width

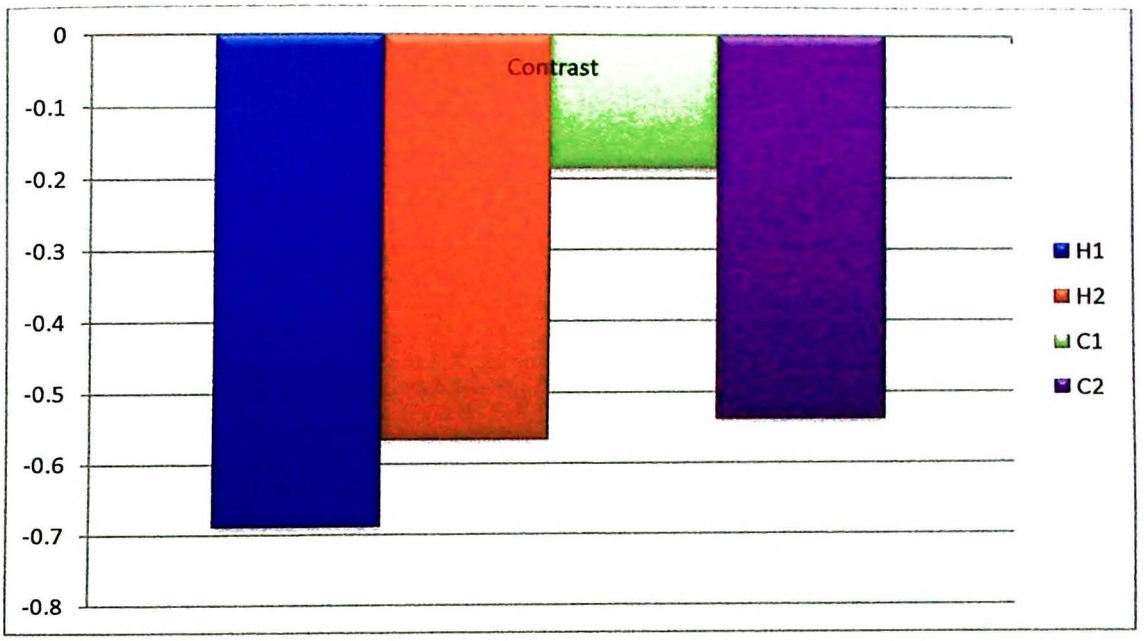

Figure 4.3 Contrast values for 20% energy window width

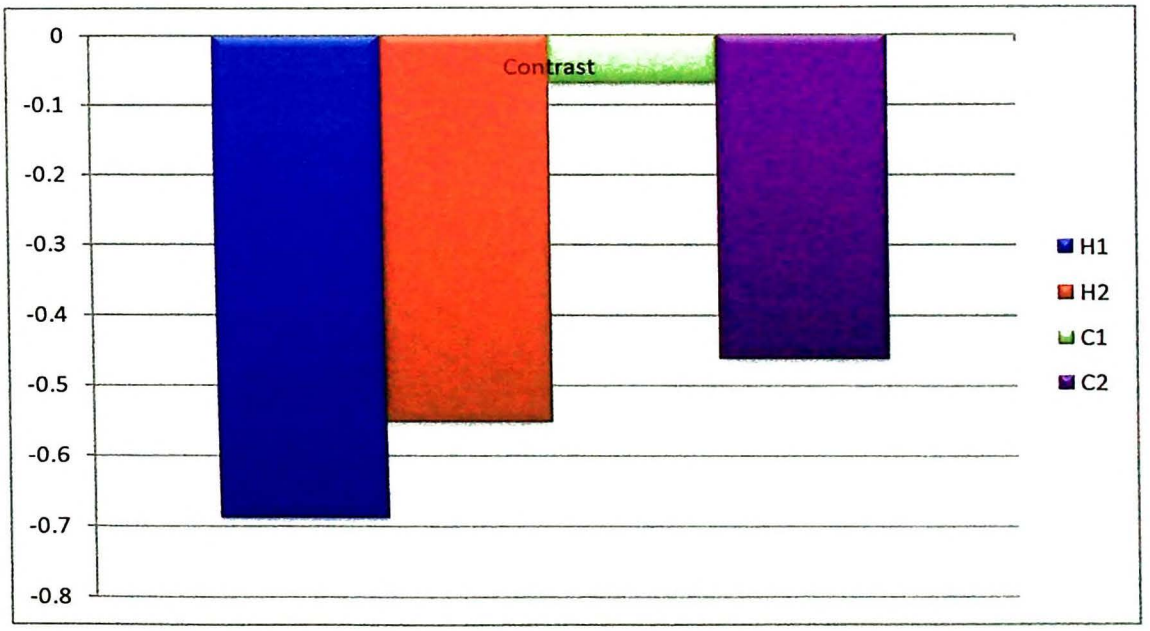

Figure 4.4 Contrast values for 30% energy window width

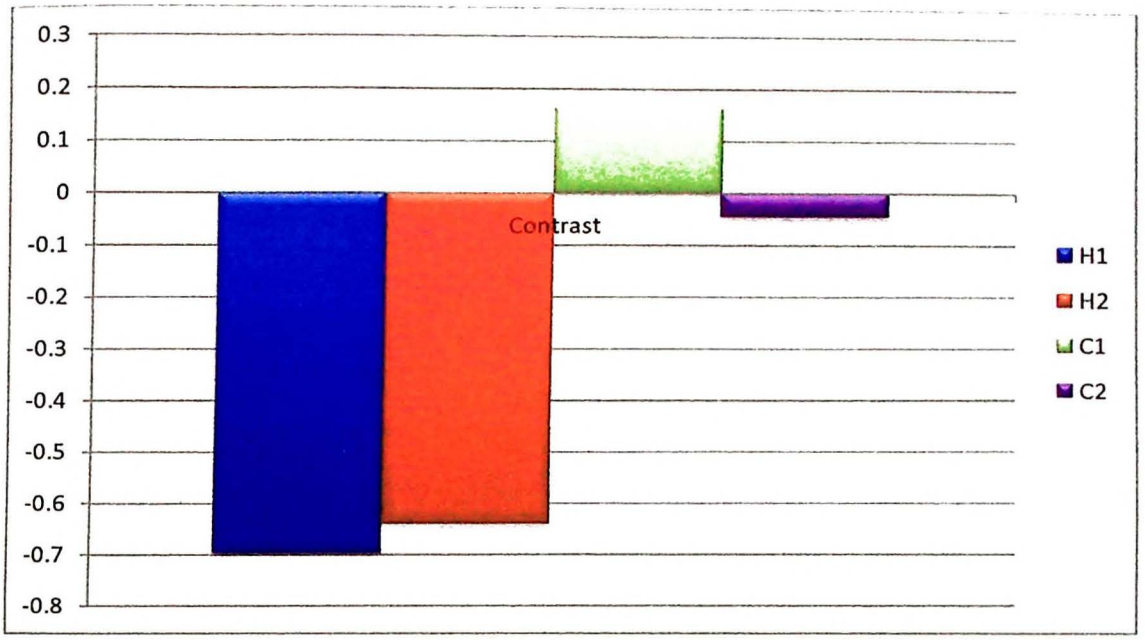

Figure 4.5 Contrast values for 40% energy window width

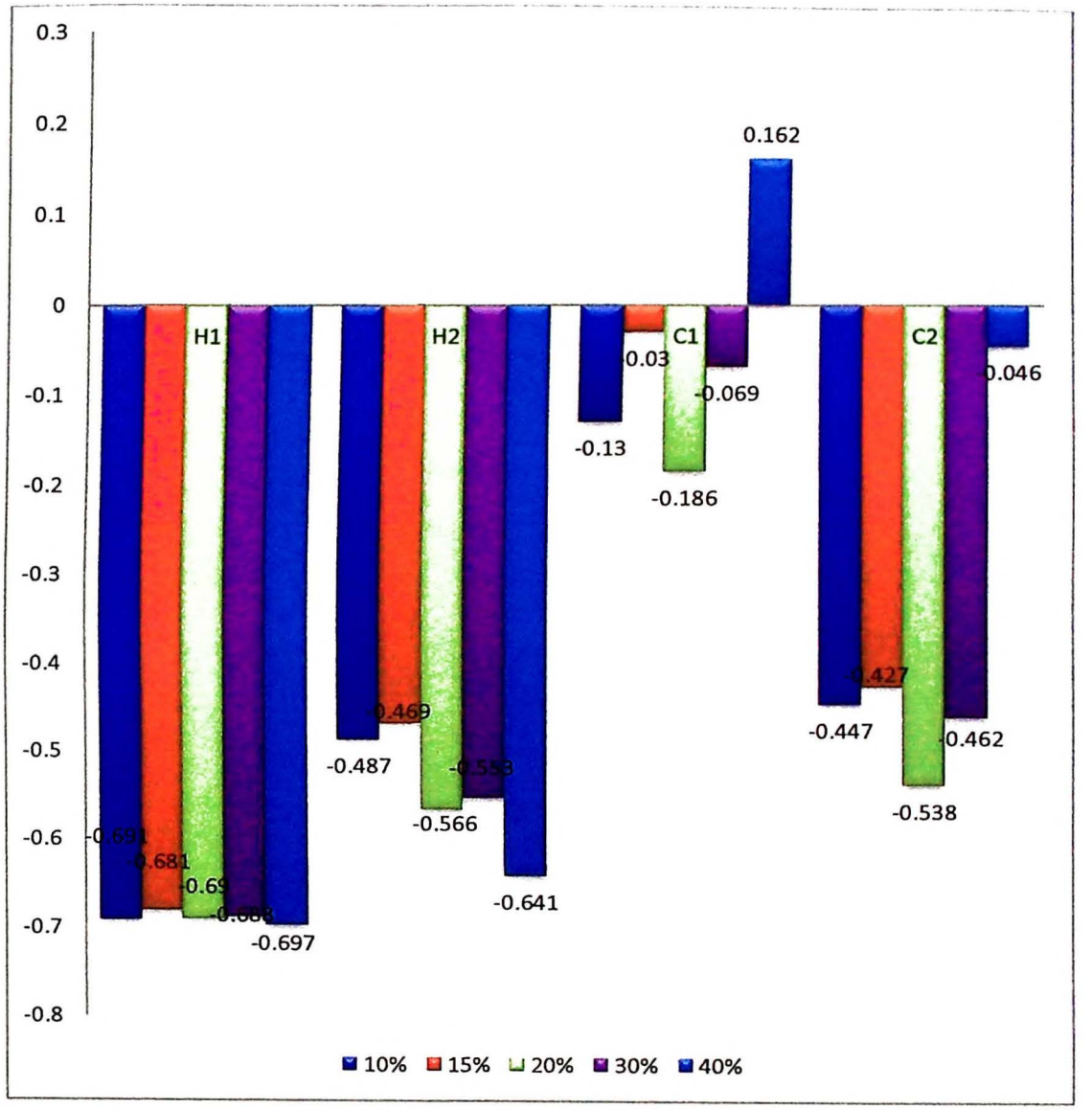

Figure 4.6 Comparison of contrast values for all five energy window widths

The SNR for each nodule of every energy window widths were calculated and the results were shown in the **Table 4.2** (can be referred at the Appendix D). The graphs of SNR for every energy window widths were shown in the **Figure 4.7**, **Figure 4.8**, **Figure 4.9**, **Figure 4.10** and **Figure 4.11**. Last but not least, the **Figure 4.12** showed the comparison of SNR for all five energy window widths.

Table 4.2 SNR values of each point for each energy window width

Energy window width (%)	Signal to noise Ratio (SNR)			
	H1	H2	C1	C2
10	4.272	2.955	7.314	10.284
15	6.196	5.015	9.763	11.686
20	3.444	2.702	6.422	11.489
30	4.115	3.972	9.748	11.494
40	3.787	3.535	5.638	11.148

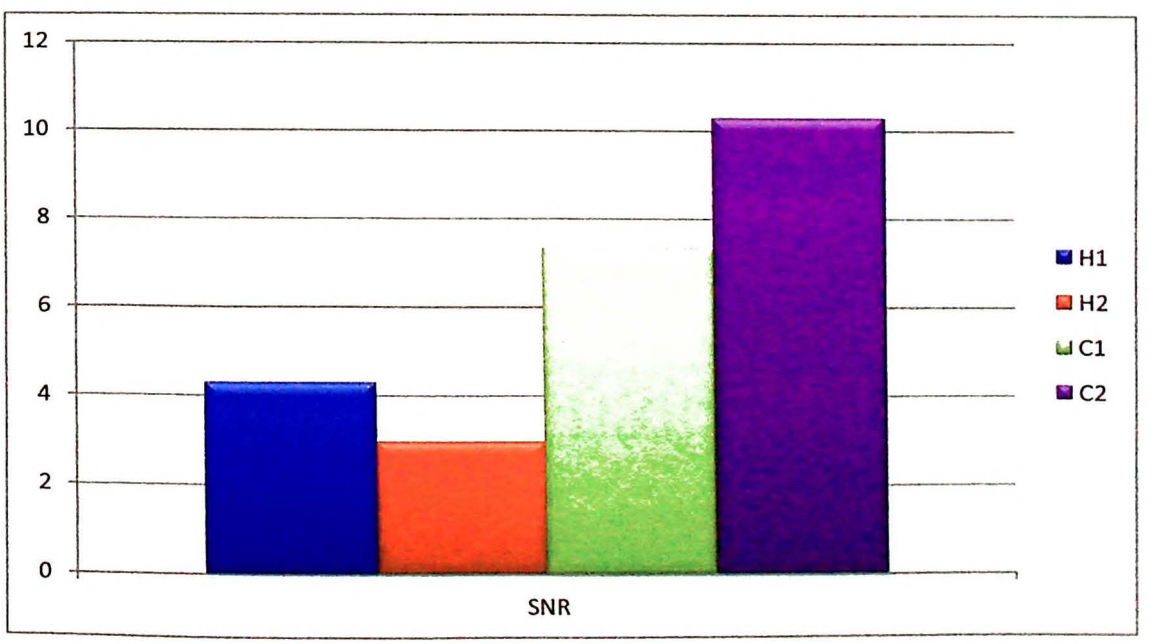

Figure 4.7 SNR values for 10% energy window width

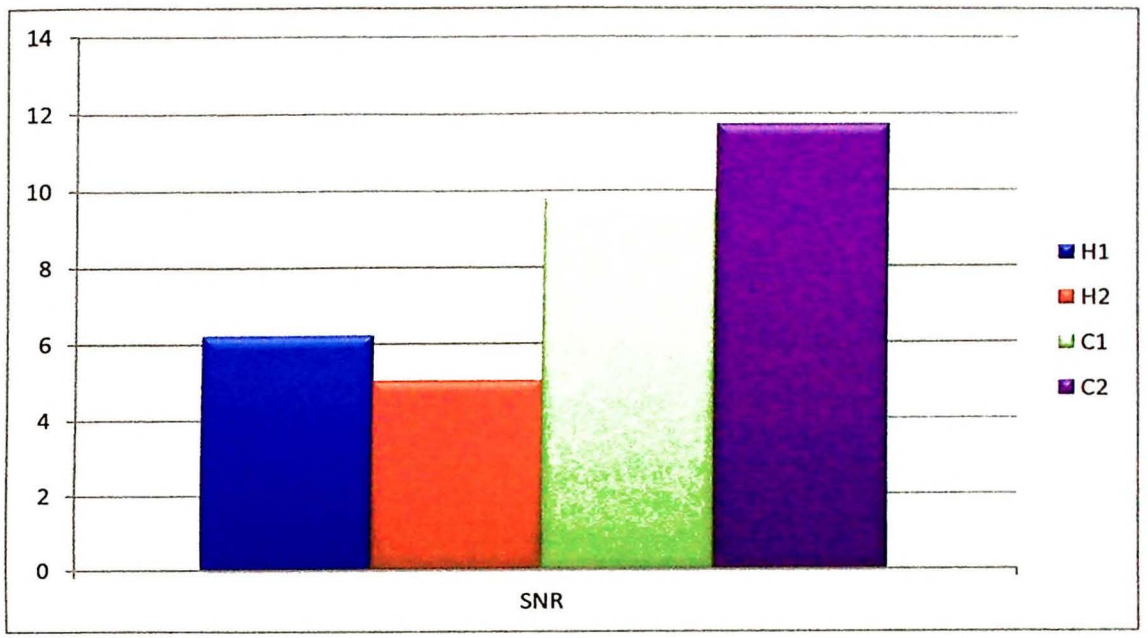

Figure 4.8 SNR values for 15% energy window width

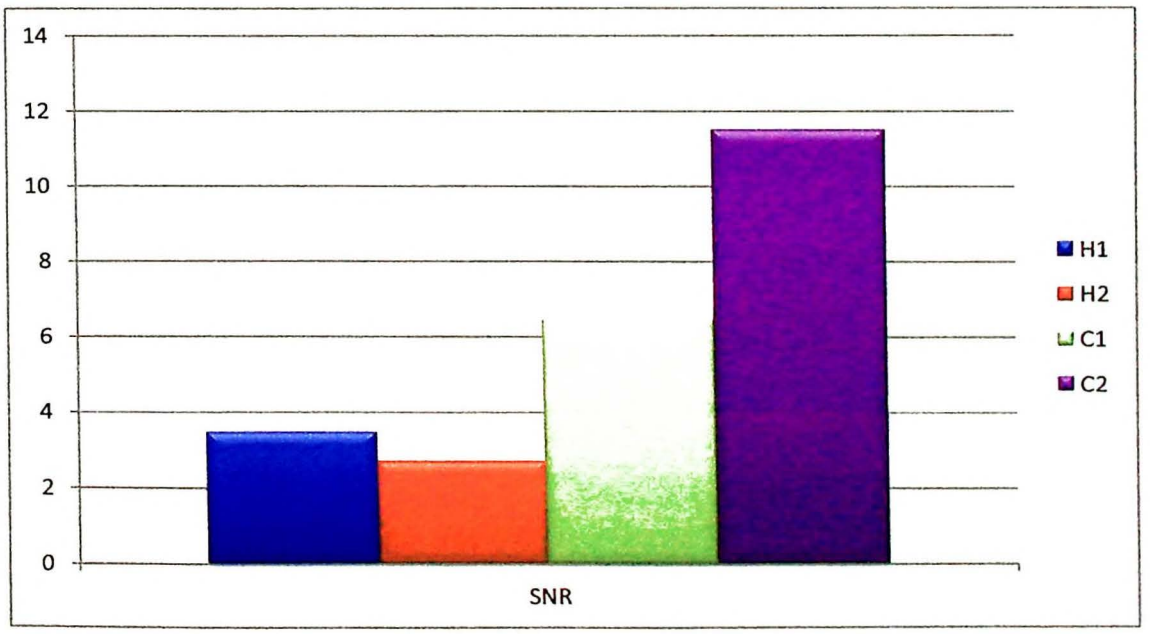

Figure 4.9 SNR values for 20% energy window width

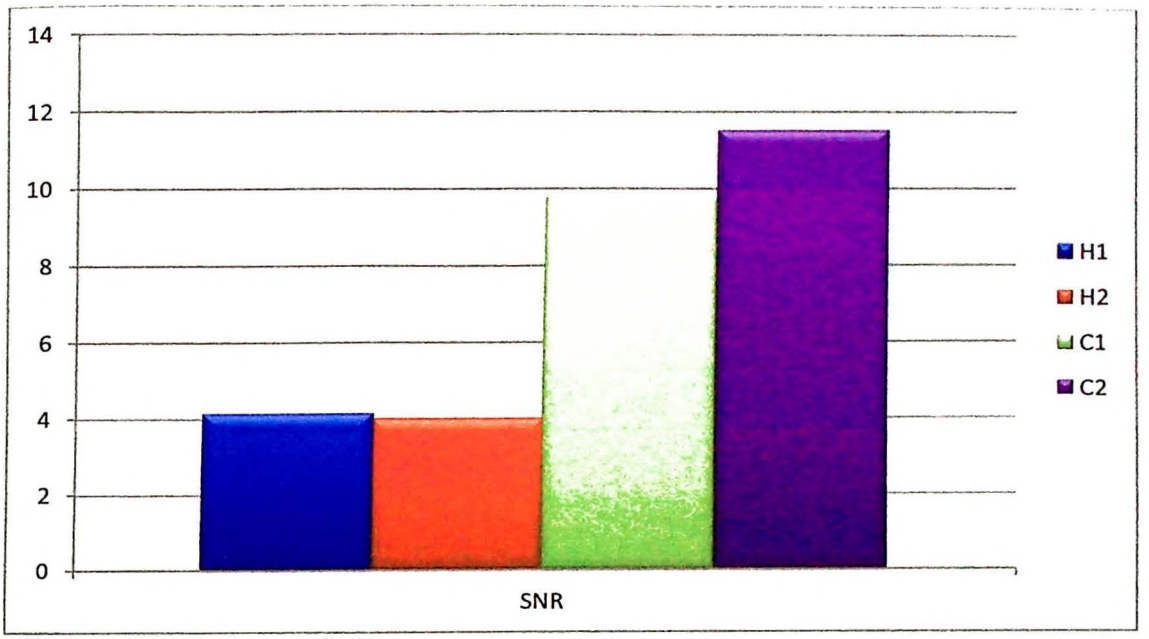

Figure 4.10 SNR values for 30% energy window width

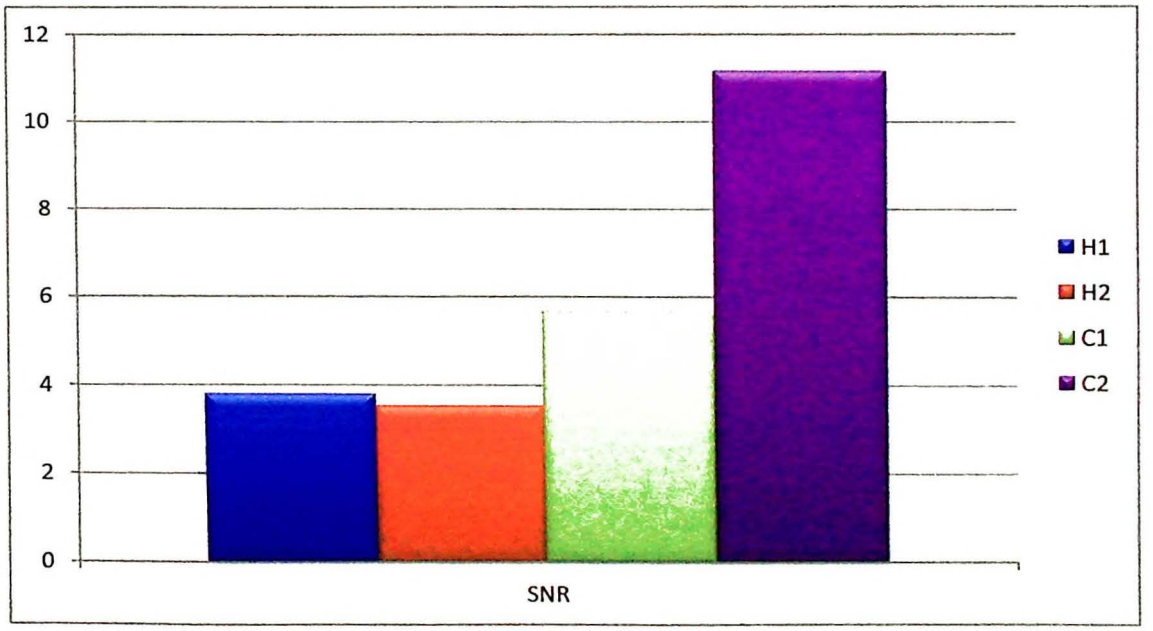

Figure 4.11 SNR values for 40% energy window width